

# Control of Nanoparticles in a Plasmachemical Reactor

Emmanuel Rotimi Sadiku<sup>1</sup>, Oluranti Sadiku-Agboola and Olusesan Frank Biotidara

*Department of Mechanical Engineering, Faculty of Engineering and the Built Environment, Tshwane University of Technology, South Africa*

Received: December 09, 2010 / Accepted: January 05, 2011 / Published: August 25, 2011.

**Abstract:** The mixture of titanium tetrachloride and oxygen for the formation of titanium nanoparticles in a plasma reactor is examined. A coupled model for the simulation and control of nanoparticle in a plasmachemical reactor with simultaneous chemical reaction, nucleation, condensation and coagulation is proposed. The population balance model describes how the particle size distribution evolves with time. The population balance model was solved numerically and the effect of the wall temperature on the average particle diameter was investigated in order to ascertain whether the model can be used to control nanoparticle size distribution. Numerical modeling was conducted in order to describe the mechanism of nanoparticle formation. Comparison was made by another software.

**Key words:** Nanoparticles, plasmachemical reactor, nucleation, coagulation, SCILAB, MATLAB.

## Abbreviations

RF	Radio frequency
Ar	Argon
CH <sub>4</sub>	Methane
NH <sub>3</sub>	Ammonia
CVD	Chemical vapour deposition
TaC	Tantalum carbide
PECVD	Plasma-enhanced vapour deposition
XRD	X-ray diffraction
BET	Brunauer Emmett Teller theory
NCD	Noncrystalline diamond
TiO <sub>2</sub>	Titanium dioxide
TiCl <sub>4</sub>	Titanium tetrachloride
O <sub>2</sub>	Oxygen
Cl <sub>2</sub>	Chlorine

## 1. Introduction

Plasma science and technology is a key research area of the 21st century. Many products, ranging from computers to energy saving lamps, depend on successful plasma processes. Plasmas are used for the creation of nanostructures with unrivalled precision

---

**Corresponding author:** Emmanuel Rotimi Sadiku, Ph.D., professor, research fields: X-ray physics and rheology of polymers and polymer composites. E-mail: sadikur@tut.ac.za.

and for functional coatings to give products superior surface properties. Plasma thermal flow is regarded as one of the multifunctional fluids with high energy density, chemical reactivity, and it is controlled by an external electromagnetic field and variable transport properties such as electrical conductivity [1]. Furthermore, the chemical reaction time is comparatively long due to the low plasma velocity. It is very important to control, precisely the plasma structure, e.g., the plasma properties, the thermo fluid fields and the induction electromagnetic fields and also the behaviours of the injected particles. Plasma chemical technology implements an in-flight evaporation of precursor. The raw materials, having the highest boiling-point and operating under various atmospheres, permits the synthesis of a great variety of nanopowders, and thus become a very reliable and efficient technology for the synthesis of nanopowders, on both laboratory and industrial scales. Plasma chemical used for nanopowders synthesis has many advantages over the alternative techniques, such as high purity, high flexibility, easy to scale-up, easy to operate and process control. In the nano-synthesis process, material is first heated up to evaporation in a plasma chemical reactor, and the vapours are

subsequently subjected to a very rapid quenching in the quench/reaction zone of the reactor. The quench gas can be an inert gas such as Ar and N<sub>2</sub> or reactive gases such as CH<sub>4</sub> and NH<sub>3</sub>, depending on the type of nanopowders to be synthesized. The nanometric powders produced are usually collected by porous filters, which are installed at some collection point, away from the plasma reactor section. Because of the high reactivity of metal powders, special attention should be given to powder pacification prior to the removal of the powder collected from the filtration section of the process.

In plasmachemical reactors, the existence of a radio frequency (RF) field, interacting with the various charged particles and surfaces, imposes several differences from classical chemical systems. From the kinetic point of view, the presence of highly excited species requires the use of state-specific data. However, Arrhenius-type extrapolations using the gas temperature, cannot describe the variation of the rate constant of electron-molecule reactions as a function of the energy of the system, since these systems decline from thermodynamic equilibrium [2]. Recent developments have permitted the accurate determination of the power that is actually consumed in reactive gas plasmas such as the silane discharge that is widely used in the microelectronic industry. Thus, there is a possibility of correlating the dissociation rate constant to the energy content of the discharge environment. Gordiets and Bertran [3] created a self-consistent global kinetic model based on simple equations that can describe the formation, growth, destruction of clusters and dust nanoparticles and plasma parameters of low-pressure RF discharges. Processes that involve the participation of charged particles diffusion, losses of cluster and dust nanoparticles were taken into account. Chen et al. [4] developed a simple but versatile atmospheric direct current mini-arc plasma source to produce nanoparticles as small as a few nanometers in dimension. They were formed by direct vapourization

of solid precursors followed by rapid quenching. Shimada et al. [5] synthesized gallium nitride nanoparticle via improved microwave plasma-enhanced chemical vapour deposition (CVD) method. Optimization of the process was achieved by manipulating the plasma operating conditions, such as antenna length, input power and pressure. Mendoza Gonzalez et al. [6] discovered that, the use of quench injection plays an important role in the final size and structure of the particles produced. Their approach was used to study the relationship between the operating parameters effect and the properties of the end products at the laboratory scale.

The main route of nanoparticle formation in the gas-phase is by a chemical reaction leading to a non-volatile product, which undergoes homogeneous nucleation followed by condensation and growth. Recently, this has become an important pathway for the industrial production of nanoparticle powders, which may be of metals, oxides, semiconductors, and various forms of carbon and which may be in the form of spheres, wires, needles, tubes, platelets or other shapes. The increased demand for nanopowders has promoted the extensive research and development of various techniques for nanometric powders. The challenges for an industrial application technology are productivity, quality controllability, and affordability. Numerical modeling is a good way to achieve a better knowledge and understanding of the process. The gas flow rates should be adjusted for the specific conditions of nanoparticles synthesis. Vorobev et al. [7] developed a simple and efficient numerical model describing the processes of nucleation, growth and transport of multi-component nanoparticles. The approach is conceptually similar to the classical method of moments but can be applied to co-condensation of several substances. The processes of homogeneous nucleation, heterogeneous growth, and coagulations due to Brownian collisions were considered in combination with the convective and diffusive transport of particles and reacting gases within

multi-dimensional geometries. The model was applied to the analysis of multi-component co-condensation of TaC nanoparticles within a dc plasma reactor. Girshick and Warthesen [8] simulated plasma-particle system for conditions of nanoparticle formation during plasma-enhanced chemical vapor deposition (PECVD) of silicon thin films. Their simulations predicted that many neutral particles are able to escape the plasma and deposit on reactor walls or a substrate before becoming negatively charged and trapped in the centre region of the plasma. Neyts et al. [9] carried out two different numerical simulation approaches to describe hydrocarbon plasmas in their applications for either nanoparticle formation in the plasma or the growth of nanostructured thin films, such as nanocrystalline diamond (NCD). A plasma model based on the fluid approach is utilized to study the initial mechanisms giving rise to nanoparticle formation in acetylene plasma. The growth of NCD was investigated by molecular dynamics simulations, describing the interaction of the hydrocarbon species with a substrate. Kolesnikov et al. [10] presented the results of controlled synthesis of alumina nanopowder in a three-jet plasmachemical reactor, where temperature and velocity distributions are controlled by the angle of impingement of the plasma jets. The flow and temperature fields for various impingement angles were measured by an enthalpy probe. The products were characterized by means of electron microscopy, XRD and BET theory analyses.

The plasma reactor system has been successfully used in the synthesis of nanopowders. The typical size range of the nano-particles produced is from 20 to 100 nm, depending on the quench conditions employed. The productivity varies from a few hundred g/h to between 3,000~4,000 g/h, according to the different materials' physical properties. Nanoparticles show novel properties compared to the bulk material of same chemistry. The small size is responsible for many changes in the thermo-physical properties. Thus, there was an increasing interest in nanomaterials. The

objective of this work is to study the effect of wall temperature on the average particle diameter in the process of nanoparticle production using population balance model. The effect of the wall temperature may influence the particle morphology, sizes, and distributions in order to control the particle size distribution under high temperature.

## 2. The Basic Description of the Process

Plasmachemical reactor uses its know-how hot plasma process to produce nanoparticles. Precursor material is atomized in a plasma arc, followed by clusterization to nanoparticles and optionally with additional plasma chemical conversion to another material than the precursor. Special precautions are followed in order to get real nanocrystals (not simply mixed phases) and to also exclude big agglomerate formation. In this process, the formation of clusters and nanoparticles in molecular gas plasma can be described as follows: As a result of dissociation of parent molecules by an electron impact and chemical reaction in the gas phase, small size clusters and radical monomers of condensable species are formed. Due to the attachment of monomers to cluster, the clusters grow further by monomer condensation and nucleate to the size of nanoparticles, which also continue to grow in size and their concentration may attain a certain cluster size value. Finally, the growth occurs mainly by coagulation and condensation occurs in the synthesis chamber where the plasma gets colder and form high-purity nanoparticles; the growth of which is stopped by gas quenching, with the relative strength of each greatly affecting the particle size and morphology. Fig. 1 shows the graphical description of the process.

### 2.1 Titanium Dioxide Formation Reaction Model

The reaction model describes the formation of Titanium dioxide ( $\text{TiO}_2$ ) nanoparticle in plasma chemical reactor. Monomers are chemically produced from low-boiling, but highly reactive precursors. The formation of  $\text{TiO}_2$  takes place by the overall reaction of

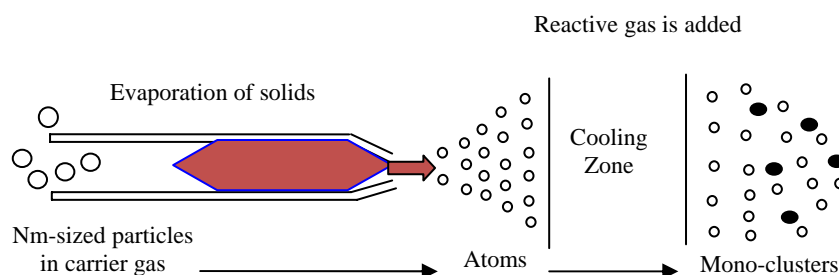


**Fig. 1** Plasma chemical synthesis of nanoparticles.

$\text{TiCl}_4$  with  $\text{O}_2$ : The size of a single  $\text{TiO}_2$  molecule (monomer) is larger than the thermodynamic critical cluster size. For this reason, chemical reaction and nucleation become indistinguishable, thereby implying that the rapid chemical reaction leads to a nucleation

burst. The  $\text{TiO}_2$  monomers coagulate leading to larger average particle size and smaller particle concentration



The mechanism of  $\text{TiO}_2$  formation is given in Fig. 2 and the simulation parameters is given in the Table 1.

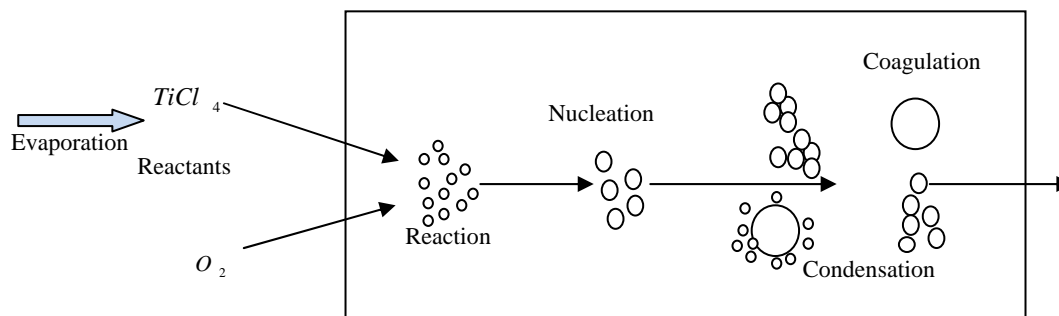


**Fig. 2** Mechanism of  $\text{TiO}_2$  formation.

**Table 1** Process model parameters used for the simulation study.

$D = 0.1 \text{ m}$	Reactor diameter
$P_0 = 101,000 \text{ Pa}$	Process pressure
$T_0 = 2,200 \text{ K}$	Inlet temperature
$T_w = 120 \text{ K}, 130 \text{ K}, 170 \text{ K}$	Wall temperatures
$Y_{10} = 0.5$	Inlet mole fraction of $\text{O}_2$ reactant
$y_{20} = 0.5$	Inlet mole fraction of $\text{TiCl}_4$ reactant
$U = 150 \text{ Jm}^{-2}\cdot\text{S}^{-1}\cdot\text{K}^{-1}$	Overall coefficient of heat transfer
$\Delta H_R = 88000 \text{ J mol}^{-1}$	Heat of reaction
$C_p = 1,615.25 \text{ mol}^{-1}\cdot\text{K}^{-1}$	Heat capacity of process fluid
$MW_g = 14.0 \times 10^{-3} \text{ kg}\cdot\text{mol}^{-1}$	Mol wt. of process fluid
$K = 11.4 \text{ m}^3\cdot\text{mol}^{-1}\cdot\text{S}^{-1}$	Reaction rate constant
$\mu = 6.5 \times 10^{-5} \text{ kg}\cdot\text{m}^{-1}\cdot\text{s}^{-1}$	Viscosity of process fluid
$P_s = \exp(-4644/T + 0.906 \log(T) - 0.00162T + 9.004) \times (101,000/760)$	Saturation pressure (Pa)
$\gamma = 0.08 \text{ N m}^{-1}$	Surface tension
$v_1 = 5.0 \times 10^{-29} \text{ m}^3$	Monomer volume
$N_{av} = 6.023 \times 10^{23} \# \text{ mol}^{-1}$	Avogadro's constant
$R = 8.314 \text{ Jmol}^{-1}\cdot\text{K}^{-1}$	Universal gas constant
$k_B = 1.38 \times 10^{-23} \text{ J}\cdot\text{K}^{-1}$	Boltzmann's constant
$so = 1.1587 \times 10^{-19}$	Surface area of monomers
$\sigma = 0.5$	Sigma

Both saturation ratio and nucleation are essential in the content of this study. The saturation ratio,  $S$  is the ratio of the component pressure,  $p$  in the mixture and the saturation vapour pressure,  $p^{sat}$  is the saturation vapour pressure,  $p^{sat}$  is the pressure required to maintain a vapour in mass equilibrium with the condensed vapour at specific temperature. When the component pressure reaches the saturation vapour pressure, the vapour starts to condense. The saturation ratio is usually very high even at high temperature under the supply of energy for chemical reaction.

$$S = \frac{P_{TiO_2}}{P_{TiO_2}^{sat}} \quad (2)$$

## 2.2 Population Balance Model

The population balance equation that consists of nonlinear partial integro-differential equation is given below, according to that described by Kalani and Christofides [11]:

$$\frac{\partial n}{\partial t} + \frac{\partial (G(v, \bar{x})n)}{\partial v} - I(v^*)\delta(v-v^*) = \frac{1}{2} \int_0^v \beta(\tilde{v}, v-\tilde{v}, \bar{x})n(\tilde{v}, t)n(v-\tilde{v}, t)d\tilde{v} - n(v, t) \int_0^\infty \beta(v, \tilde{v}, \bar{x})n(\tilde{v}, t)d\tilde{v} \quad (3)$$

The first term on the left hand side of Eq. (3) describes the change in the number concentration of particle, the volume interval  $v$ ,  $v+dv$ ,  $n(v, t)$  denotes the particle size distribution function,  $v$  is particle volume,  $t$  is time, the third term on the left hand side accounts for the formation of new particles of critical volume,  $v^*$  by nucleation rate,  $I$ .  $I(v^*)\delta(v-v^*)$ , and it also accounts for the gain and loss of particles by condensation. The second term on the left hand side gives the loss or gain of particles by condensational growth.  $I(v^*)$  and  $\beta(\tilde{v}, v-\tilde{v}, \bar{x})$  are the nonlinear scalar functions and  $\delta$  is the standard Dirac function.

The mass and energy balance model which predicts the spatio-temporal evolution of the concentrations of species and temperature of the gas phase given by Kalani and Christofides [11] takes the following form:

$$\frac{d\bar{x}}{dt} = \bar{f}(\bar{x}) + \bar{g}(\bar{x})u(t) + \bar{A} \int_0^\infty a(\eta, v, x)dv \quad (4)$$

where  $\bar{x}(t)$  is an  $n$ -dimensional vector of state variables that depends on space and time,  $\bar{A}$  is constant matrix,  $\bar{f}(\bar{x})$ ,  $\bar{g}(\bar{x})$ ,  $a(\eta, v, x)$  are nonlinear vector functions,  $u(t)$  is the time varying manipulated input (e.g. wall temperatures,  $T_{W_1}$  and  $T_{W_2}$ ). The term  $\bar{A} \int_0^\infty a(\eta, v, x)dv$  accounts for mass and heat transfer from the continuous phase to all the particles in the population. The gain and loss of particles by Brownian coagulation is described by the first and second terms on the right hand side of Eq. (4) respectively.

The simulation domain is assumed to be radially large, thus the population balance model was reduced to the first three moments under the assumption of log-normal size distribution.

## 2.3 Moment Model

It is assumed that the aerosol size distribution can adequately be represented by log-normal function which is described as:

$$n(v, t) = \frac{1}{3v} \frac{1}{\sqrt{2\pi} \ln \sigma} \exp \left[ -\frac{\ln^2(v/v_g)}{18 \ln^2 \sigma} \right] \quad (5)$$

where  $v_g$ , is the geometric average particle volume and  $\sigma$  is the standard deviation. The  $k$ th moment of the distribution is defined as:

$$M_k(t) = \int_0^\infty v^k n(v, z, t) dv \quad (6)$$

According to the properties of a log-normal function, any moment can be written in terms of  $M_0$ ,  $v_g$ , and  $\sigma$  as follows:

$$M_k = M_0 v_g^k \exp \left( \frac{9}{2} k^2 \ln^2 \sigma \right) \quad (7)$$

If Eq. (7) is written for  $k = 0, 1$ , and  $2$ , then  $v_g$  and  $\sigma$  can exactly be expressed in terms of the first three moments of the distribution according to the following relations:

$$\ln^2 \sigma = \frac{1}{9} \ln \left( \frac{M_0 M_2}{M_1^2} \right) \quad \text{and} \quad v_g = \frac{M_1^2}{M_0^{3/2} M_2^{1/2}} \quad (8)$$

### 3. Discussion of Results

In this section, the results of several simulation runs of uncontrolled process in high temperature reactor leading to particle nucleation and growth were presented. They give key insights into the interplay of various coagulation mechanisms that take place in the process. This will lead to the formulation of a meaningful control configuration which is the selection of manipulated variable. An advanced understanding of parameters that determine the formation of particle is crucial for the successful simulation of the process, hence choosing meaningful range of input parameters should be done with great care. Initial parameters were

chosen close to the data published in literature for the same process. The process model of the system was numerically solved by using Simulink, which is a part of (Matlab) software environment. According to Ref. [12], it is an interactive computing package for simulating and analysing differential equations, mathematical models and controlling dynamic systems. It was established that through numerous simulations, the results obtained are accurate in the sense that it was further verified with different software (Scilab) and the results are identical.

Fig. 3 shows the comparison of some results. Scilab is software used for numerical mathematics and

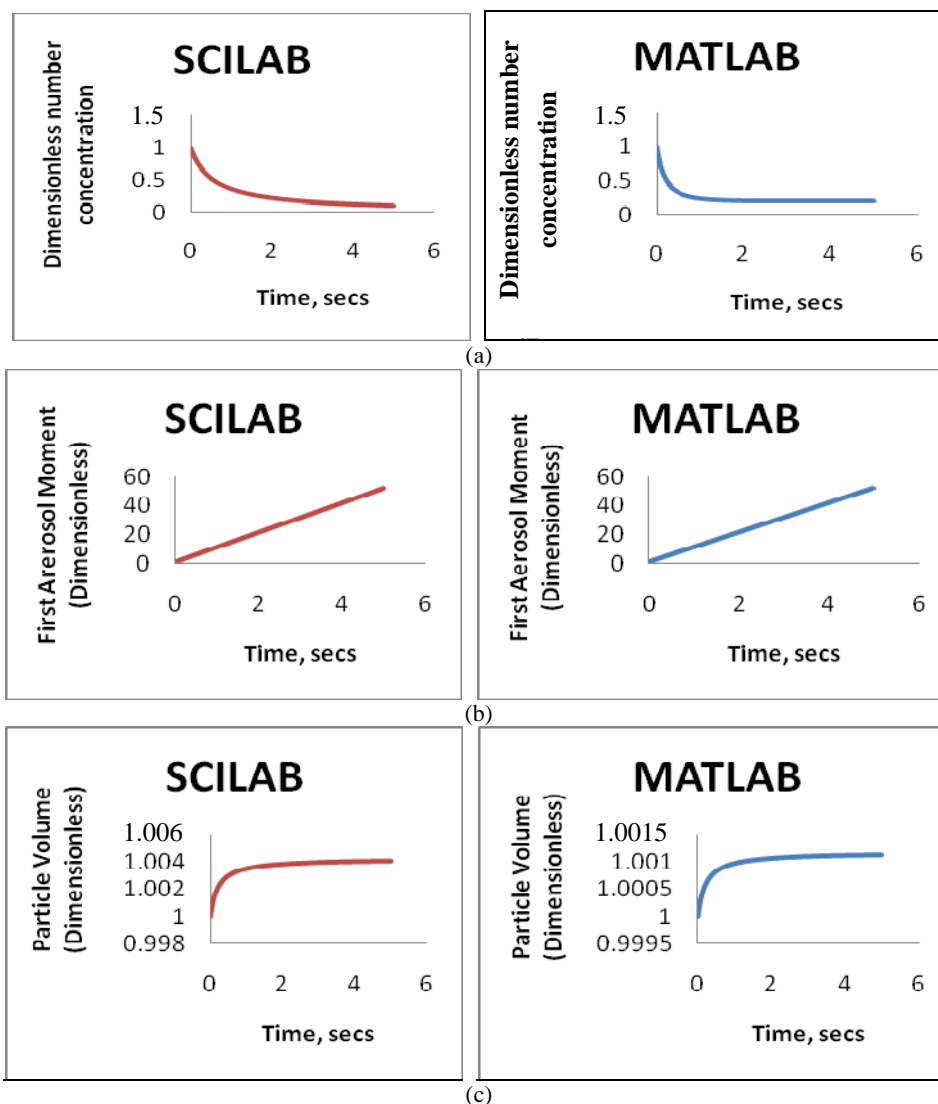


Fig. 3 Comparison of dimensionless number concentration (a), first aerosol moment (dimensionless) (b) and particle volume (dimensionless) (c) as functions of time respectively.

scientific visualization. It gives intermediate steps in solving complicated problems. Being compatible with Matlab, the comparisons of results obtained from Scilab and Matlab are given below. The softwares, Scilab and Matlab give similar results for the evolution of the first three moments of particle size distribution. As particles collide and coagulate, their number concentration decreases. This is revealed in the zeroth moment  $M_0$ . As the flow evolves,  $M_0$  decreases while the first aerosol moment is increasing as shown in Fig. 3. Since the objective is to investigate if the population balance model can control nanoparticle growth with desired particle distribution in the plasmachemical reactor, the effect of wall temperature on average particle diameter was also studied. It is a variable that could be used in industry to control the particle size distribution.

At high temperature, aerosol process for synthesis of titania nanopowders was demonstrated by elucidating the influence of temperature and concentration of precursors on particle size. In this model, the initial temperature of the gas mixture entering the reactor is 2,200 K. At this temperature,  $\text{TiCl}_4$  is added to  $\text{O}_2$  for the chemical reaction in Eq. (1) to take place. However  $\text{Cl}_2$  does not have effect on the formation of  $\text{TiO}_2$  since the source for  $\text{TiO}_2$  production is based on the forward reaction of  $\text{TiCl}_4$  and  $\text{O}_2$ .  $\text{Cl}_2$  gas does not take part in the reaction as raw material, it is just a product. Therefore the concentration of  $\text{Cl}_2$  has no influence on

the rate of formation of  $\text{TiO}_2$ . But the oxidation was successful because it brought the reacting gases together at suitable temperature which provides suitable nuclei on which particle was formed. Since the initial temperature is high, the saturation vapour pressure after oxidation becomes high. When oxidation is completed and the process temperature and dimensionless temperature start to decrease, the saturation ratio increased constantly until it reached unity (1). Figs. 4 and 5 display the steady-state profile of the saturation ratio and dimensionless temperature against time.

Fig. 6 shows the distribution of average particle diameter with process time. Average particle diameter in the plasmachemical reactor increases with increase process time. Fig. 7 shows the variation of reactor wall temperature on average particle diameter. This was done in order to characterize the effect of the wall temperature profile on the process. It can be seen from Fig. 7, that the increase in the wall temperature ( $T_w$ ) results to an increase in the average particle diameter. At  $T_w = 170$  K, the average particle diameter is 252 nm, while at  $T_w = 130$  K and 120 K, the average particle diameter are 35 nm and 26 nm respectively. Fig. 8 gives the plot of the average particle diameter,  $d_p$  as a function of the wall temperature. From the Fig. 7 and Fig. 8, it is clear that the wall temperature is a variable that has significant effect on the average particle diameter. In the numerical investigation of the

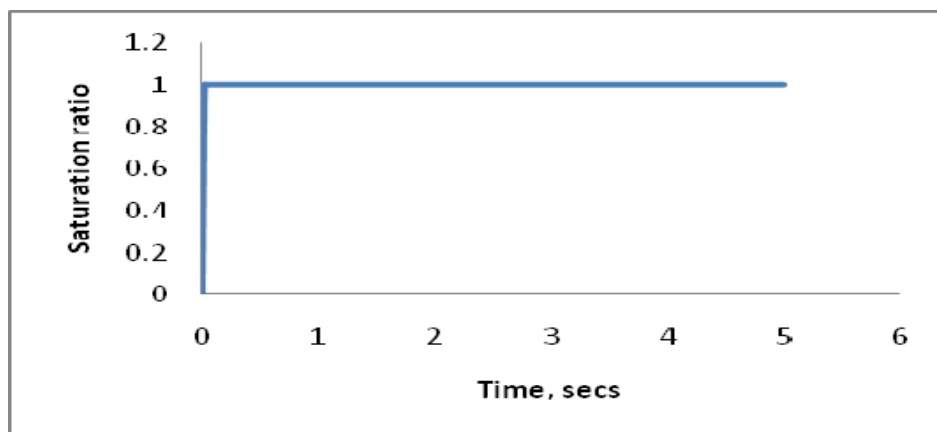


Fig. 4 Steady state profile of the saturation ratio against time (s).

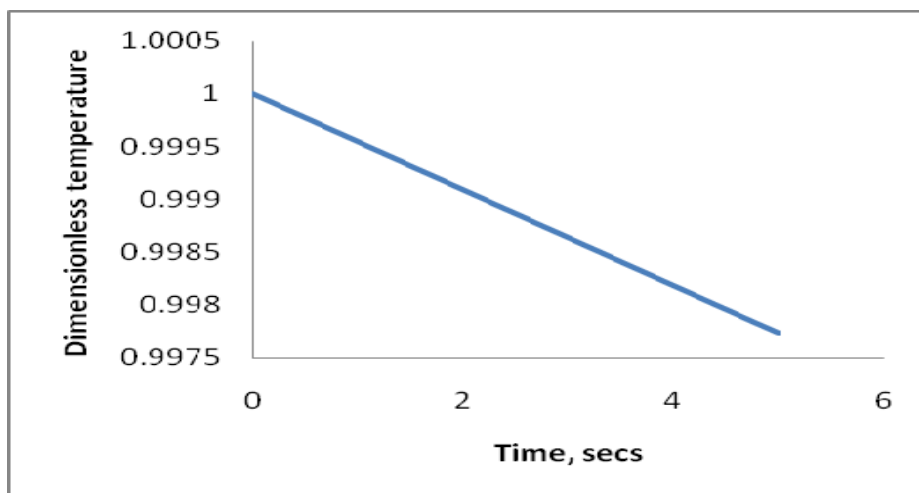


Fig. 5 Steady state profile of dimensionless temperature against time (s).

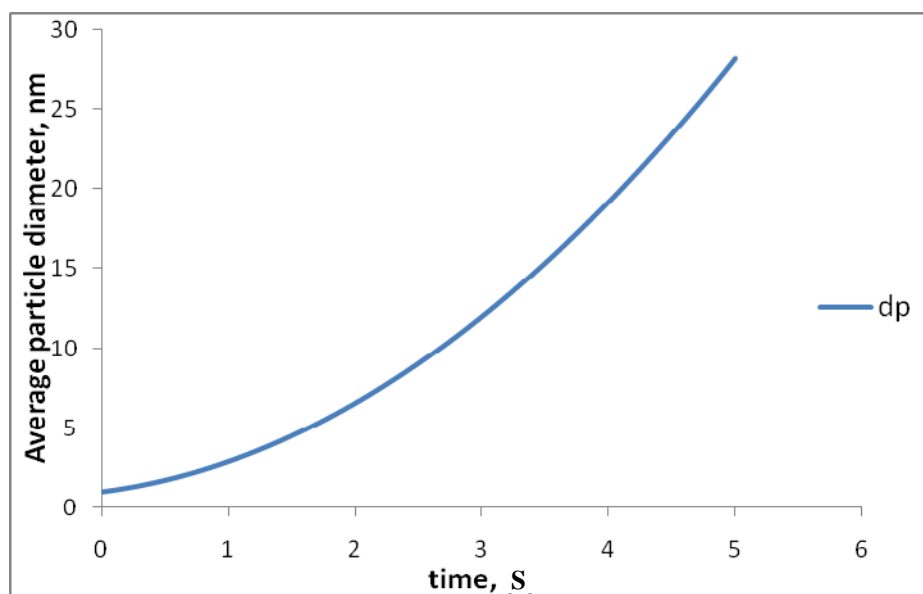


Fig. 6 Steady state profile of average particle diameter against time (s).

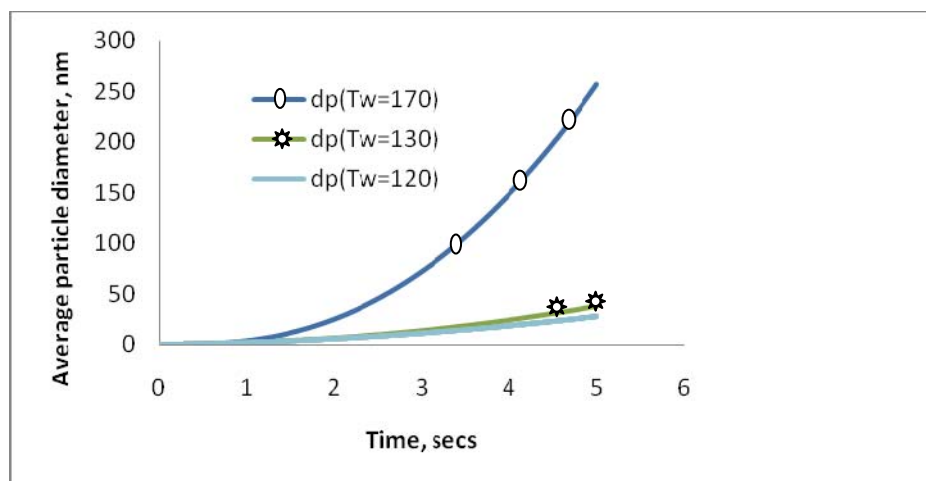
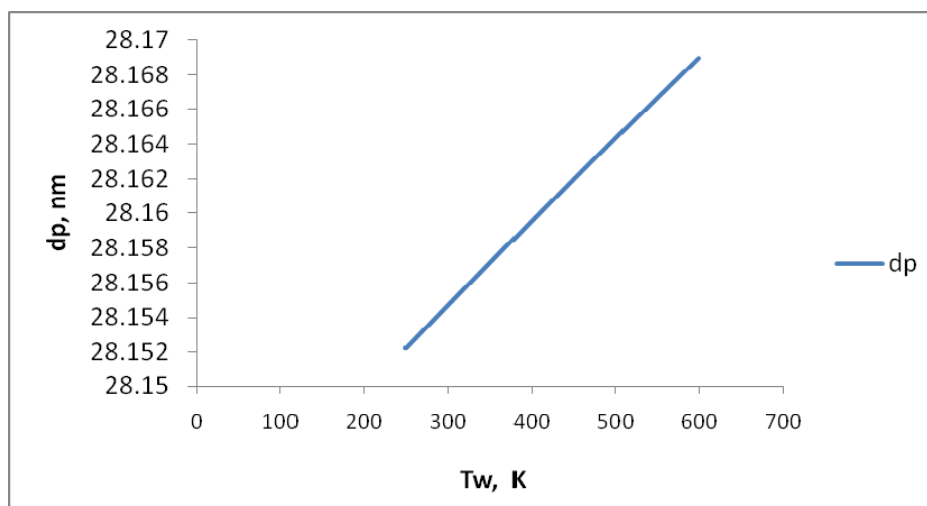


Fig. 7 Variation of reactor wall temperature on average particle diameter against the time (s).



**Fig. 8** Variation of reactor wall temperature on average particle diameter against time (s).

reactor wall temperature on particle growth, it was found that the particle size increases with increasing wall temperature the particle size distribution in a plasmachemical reactor in a high temperature condition. The accuracy with methods of moment was considered and it tracked only the moment of size distribution which can be used to control nanoparticle average diameter. The population balance model was solved numerically and the influence of wall temperature was investigated in order to ascertain whether the model can be used to control nanoparticle size distribution. Based on the sensitivity of wall temperature on the particle diameter  $d_p$ , the model can thus be used to control the particle size distribution.

## References

- [1] M. Shigeta, H. Nishiyama, Numerical analysis of metallic nanoparticle synthesis using RF inductively coupled plasma flows, *J. Heat Transfer*. 127 (2005) 1222-1231.
- [2] N. Spiliopoulos, D. Mataras, D.E. Rapakoulias, Arrhenius-like behaviour in plasma reactions, *Appl. Phys. Lett.* 71 (1997) 605-607.
- [3] B.F. Gordiets, E. Bertran, A self-consistent model for the production and growth of nanoparticles in low-temperature plasma, *Russian Journal of Physical Chemistry* 2 (2008) 315-328.
- [4] J. Chen, G. Lu, L. Zhui, R.C. Flagan, A simple and versatile mini-arc plasma source for nanocrystal synthesis, *J. Nanoparticle Research* 9 (2007) 203-213.
- [5] M. Shimada, W. Wang, K. Okuyama, Synthesis of gallium nitride nanoparticles by microwave plasma-enhanced CVD, *J. Chemical Vapour Deposition* 16 (2010) 151-156.
- [6] N.Y. Mendoza-Gonzalez, B.M. Goortani, V.P. Proulx, Numerical simulation of silica nanoparticles production in an RF plasma reactor: effect of quench, *Material Science and Engineering* 27 (2007) 1265-1269.
- [7] A. Vorobev, O. Zikanov, P. Mohanty, Modelling of the in-flight synthesis of TaC nanoparticles from liquid precursor in thermal plasma jet, *J. Phys. D: Appl. Phys.* 41 (2008) 1-15.
- [8] S. L. Girshick, S.J. Warthesen, Nanoparticles and plasmas, *Pure Appl. Chem.* 78 (2006) 1109-1116.
- [9] E. Neyts, M. Eckert, M. Mao, A. Bogaerts, Numerical simulation of hydrocarbon plasmas for nanoparticle formation and the growth of nanostructured thin films, *Plasma Phys. Control. Fusion* 51 (2009) 1-8.
- [10] A.V. Kolesnikov, N. Alexeev, A. Samokhin, Controlled synthesis of alumina nanoparticles in a reactor in self-impinging plasma jets, *International Journal of Chemical Reactor Engineering* 2 (2007) A95.
- [11] A. Kalani, P.D. Christofides, Simulation, estimation and control of size distribution in aerosol processes with simultaneous reaction, nucleation, condensation and coagulation, *Computers and Chemical Engineering* 26 (2002) 1153-1169.
- [12] E.L. Sergey, *Engineering and Scientific Computation Using Matlab*, Rochester Institute of Technology, Wiley Interscience, New Jersey, 2003, p. 172.